E.-F. Markus Henke, Katherine E. Wilson, Iain A. Anderson

Entirely soft dielectric elastomer robots

Erstveröffentlichung in / First published in:

SPIE Smart Structures and Materials + Nondestructive Evaluation and Health Monitoring. Portland, 2017. Bellingham: SPIE, Vol. 10163 *[Zugriff am: 02.05.2019].*

DOI: https://doi.org/10.1117/12.2260361

Entirely soft dielectric elastomer robots

E.-F. Markus Henke, Katherine E. Wilson, Iain A. Anderson

E.-F. Markus Henke, Katherine E. Wilson, Iain A. Anderson, "Entirely soft dielectric elastomer robots," Proc. SPIE 10163, Electroactive Polymer Actuators and Devices (EAPAD) 2017, 101631N (10 May 2017); doi: 10.1117/12.2260361

SPIE.

Event: SPIE Smart Structures and Materials + Nondestructive Evaluation and Health Monitoring, 2017, Portland, Oregon, United States

Entirely soft dielectric elastomer robots

E.-F. Markus Henke[a,b], Katherine E. Wilson[a], and Iain A. Anderson[a,c,d]

[a]Biomimietics Lab, Auckland Bioengineering Institute, University of New Zealand, 70 Symonds Street, Auckland 1010, New Zealand
[b]Institute of Solid State Electronics, TU Dresden, 01062 Dresden, Germany
[c]StretchSense Ltd, 114 Rockfield Rd, Penrose, Auckland, New Zealand
[d]The Department of Engineering Science, University of Auckland, 70 Symonds Street, Auckland, New Zealand

ABSTRACT

Multifunctional Dielectric Elastomer (DE) devices are well established as actuators, sensors and energy harvesters. Since the invention of the Dielectric Elastomer Switch (DES), a piezoresistive electrode that can directly switch charge on and off, it has become possible to expand the wide functionality of DE structures even more. We show the application of fully soft DE subcomponents in biomimetic robotic structures.
It is now possible to couple arrays of actuator/switch units together so that they switch charge between themselves on and off. One can then build DE devices that operate as self-controlled oscillators. With an oscillator one can produce a periodic signal that controls a soft DE robot – a DE device with its own DE nervous system. DESs were fabricated using a special electrode mixture, and imprinting technology at an exact pre-strain. We have demonstrated six orders of magnitude change in conductivity within the DES over 50% strain. The control signal can either be a mechanical deformation from another DE or an electrical input to a connected dielectric elastomer actuator (DEA). We have demonstrated a variety of fully soft multifunctional subcomponents that enable the design of autonomous soft robots without conventional electronics. The combination of digital logic structures for basic signal processing, data storage in dielectric elastomer flip-flops and digital and analogue clocks with adjustable frequencies, made of dielectric elastomer oscillators (DEOs), enables fully soft, self-controlled and electronics-free robotic structures.
DE robotic structures to date include stiff frames to maintain necessary pre-strains enabling sufficient actuation of DEAs. Here we present a design and production technology for a first robotic structure consisting only of soft silicones and carbon black.

Keywords: Soft Robotics, Dielectric Elastomer Actuators, Dielectric Elastomer Switches, Dielectric Elastomer Oscillators, Biomimetics

1. INTRODUCTION

Increasingly close interaction between human beings and robots has resulted in fundamentally changed requirements for robotic development and design. In past decades the main purpose of robots was to support and automate production processes, performing exact and repetitive tasks. But alongside the development of new production technologies and improvement of IT and control technology, the vision of robots as systems for assisting our everyday life has emerged. For instance, they can provide help for patients and the disabled as rehabilitation supports. These tasks require a close interaction between the robotic system and the human being. A conventional robot, made of stiff and bulky components, can not only endanger the user by inadequate movements, but also lower the psychological acceptance. To overcome these disadvantages of conventional robot design, the development of soft robots is of vast interest in the scientific community. In order to increase usability, lower the risk of injuries during interaction and to enhance the acceptance by users, it is necessary to substitute commonly used mechanical construction materials with soft materials, such as silicones. Materials are commonly defined as *soft* if their YOUNG's-modulus is within a range of $Y = 1 \times 10^4$ MPa...1×10^9 MPa, or

Further author information: (Send correspondence to E.-F. M. H.)
E.-F. M. H.: E-mail: m.henke@auckland.ac.nz, Telephone: +64 9 373 6543

Electroactive Polymer Actuators and Devices (EAPAD) 2017, edited by Yoseph Bar-Cohen, Proc. of SPIE
Vol. 10163, 101631N · © 2017 SPIE · CCC code: 0277-786X/17/$18 · doi: 10.1117/12.2260361

as *stiff*, if $Y = 1 \times 10^9$ MPa...1×10^{12} MPa.[1,2] The main challenge is to integrate or substitute common sensor, actuator and computing structures into a soft system.

Presently, the vast majority of soft robots use pneumatics[3–5] or hydraulics[6] for actuation purpose, but also variable length tendons[7] and shape memory alloys[8] are used. The actuators themselves are soft but need large external power sources and control units. That complicates making pneumatically and hydraulically driven robots autonomous and to integrate all necessary subunits in the soft robotic structure.

The integration of sensory functionalities in soft structures is even more challenging. Although there are currently promising developments in flexible and stretchable electronics,[9] most conventional sensory technologies are not suited for integration into soft structures, since they are based on stiff semiconductor technologies. This interferes with the integration of computational functionality, power electronics and energy storage and supply into soft structures.[10]

Although several approaches suit certain formulated[10] requirements for soft robots, until now none has shown the capability to meet all requirements. Even some very recent studies[6,11–13] use commonly known, conventional technologies comprising non-compliant structures, either as external or internal parts of the entire system. TAn example of an autonomous robotic structure is Octobot,[14] driven by decomposing reactions of fluidic propellants and the use of fluidic signal processing. We are developing an entirely soft robotic actuator that is able to be driven by integrated DE electronics, which is also suitable to be produced in modern production technologies such as 3D-printing.

Dielectric elastomers can be used as sensors, actuators, information processors, charge control, power electronics and energy harvesting. DEs were first described as actuators for large actuation[15] and were desired to be the next generation of artificial muscles.[16] They belong to the material class of electro active polymers (EAPs) and their mechanical characteristics are very similar to biological muscles.[17] DEs also possess multifuntional properties;[18] they can be used to produce large actuation,[17,19,20] can be used as sensors for large strain,[21–25] for charge control,[26–28] as power generators[29] and even as signal processors.[30–32] These properties make DEs perfect for the development of a total new class of entirely soft, autonomous robots.

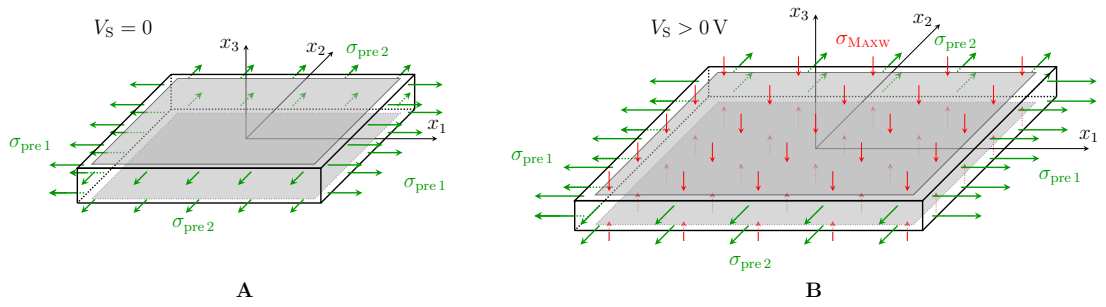

Figure 1. Basic functionality of a dielectric elastomer as actuator, pre-strained by constant biaxial pre-stresses $\sigma_{pre\,i}$ in its initial state (A) and in its actuated state caused by a MAXWELL-stress σ_{Maxw} generated by a supply voltage V_S (B).

DEs are best known for their applications in actuators. Figure 1 depicts the principle functionality. DEAs consists of thin compliant dielectric membranes, typically made of silicones or acrylic tape of several 10 µm thickness, covered with compliant electrodes on their top and bottom side. To enable actuators with large actuation, it is necessary to pre-strain the membrane in directions x_1 and x_2 (figure 1A) by an external pre-strain resulting in a stress $\sigma_{pre\,i}$. This pre-strain generates a three dimensional stress state. By applying a voltage of typically $V_S > 3000$ V to the compliant electrodes, an additional stress σ_{Maxw}, the MAXWELL-stress, occurs in direction x_3 and changes the three dimensional strain state. To reach equilibrium in its strain energy density the membrane elongates along x_1 and x_2 (figure 1B).

The actuation under constant pre-strain is proportional to the applied Voltage V_S:

$$\Delta x_i \propto \varepsilon_0 \varepsilon_r \frac{V_S^2}{d^2}, \tag{1}$$

where ε_0 and ε_r are the absolute and relative permittivity and d is the thickness of the membrane.[33] Figure 1C depicts an example actuator pre-strained in PMMA frames at different supply voltages V_S. The PMMA frames are essential to maintain the necessary pre-strain within the membrane. This causes the conflict between a soft actuator, capable of large actuation, and its stiff frame that is needed to maintain its functionality. This problem has to be solved to enable fully soft DE robots.

2. DESIGN OF FULLY SOFT ROBOTIC STRUCTURE MAINTAINING PRE-STRAIN

Most to date presented actuators, switches, logic gates, oscillators and crawling robots relied on stiff frames, made of PMMA to maintain the necessary pre-strain in their DEAs. Figure 2 depicts a DEO that can drive bioinspired robots.[34,35] It possesses soft dielectric components but still needs a stiff PMMA frame to maintain pre-strain. The combination of soft multifunctional DE membranes with stiff frames is counter-productive and, although widely used and accepted, a main obstacle to integrate high-performance DE components into fully soft robots. To overcome this issue, it is necessary to design a fully soft structure capable of maintaining pre-strain in DE membranes to enable large actuation for movement, signal generation and processing. We present the design of a simple bendable silicone skeleton possessing anisotropic bending stiffness, that is capable of maintaining a sufficient pre-strain in a silicone membrane and is still able to generate large bending and actuation.

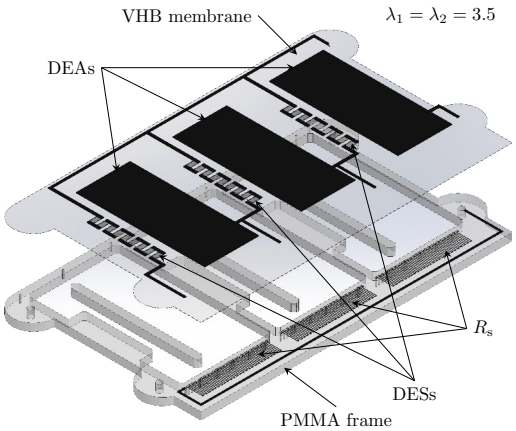

Figure 2. Explosive representation of a DEO consisting of a soft, pre-strained membrane made of VHB and a stiff supportive frame maintaining the necessary pre-strain for sufficient actuation to trigger the embedded DESs.

2.1 Design of a fully soft crawling structure

The idea for a first fully soft demonstrator was a crawling structure consisting of a simple silicone skeleton bonded to a DEA and able to change its curvature upon an applied input voltage (figure 3). This design represents a further development of dielectric elastomer minimum energy structures (DEMES).[36] Such structures usually consist of pre-strained VHB membranes glued to thin, stiff PET frames which can bend in a certain shape. DEMES adopt a deformation state of minimum energy and can generate large actuation usually by bending. A similar design is possible by using soft supportive structures. Figure 3A depicts the principle design of the crawling structure. An equibiaxially pre-strained silicone membrane is bonded to a silicone structure with anisotropic bending stiffness. The pre-strain within the membrane bends the whole structure along its softer axis. By applying a high voltage to the compliant electrodes, the bending curvature of the structure changes (figure 3B). This is because the silicone skeleton is soft, but still contains enough elastic deformation energy

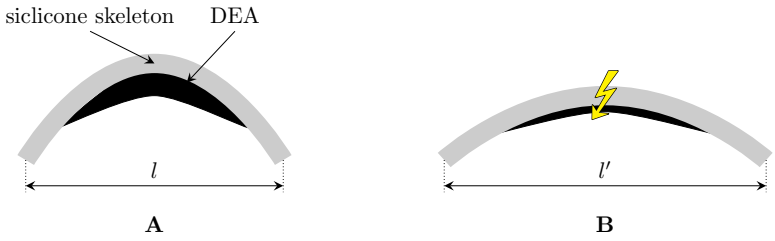

Figure 3. Basic design of entirely soft DE crawling structure. (A) Pre-strained DE membrane bends anisotropic bending stiffness structure. The initial length l is defined as distance between the contact points to the floor. (B) The bending curvature can be adjusted by applying a suitable high voltage. Changing the bending curvature results in a increase in length. The activated length is l', the stepsize $\Delta l = l' - l$.

density to perform an actuation upon a voltage induced stress reduction in the DEA. The change in bending curvature can then be translated into a crawling motion. If l is the initial length of the structure and l' the length the structure adopts upon a high input voltage, then every actuation potentially is able to move the whole structure by the distance $\Delta l = l' - l$. One has to mention that Δl is not necessarily the step size, since the contact points of the structure may slip at a surface. Furthermore, Δl depends not only on the absolute value of applied voltage but also on the frequency, because the silicone structure possesses a certain mass and, hence, resonance effects. The maximum speed of the structure can be estimated by the frequency.

2.2 Materials and methods

The production of silicone based DEAs is more challenging than the production of VHB based ones. This is mainly because of the fact that VHB is commercially available as roll material and silicones usually come as liquid or paste-like raw materials that have to be cast and cured to membranes of a desired thickness. To overcome that additional production step, WACKER have developed off-the-shelf silicone films that come in sheets or on roll, suitable for DE production. We used Wacker Elastosil 2030 films of an initial thickness of $t_0 = 100\,\mu m$. The silicone skeleton was mould cast using a liquid PDMS silicone (Sylgard 184, by Dow Corning). To bond the DEA to the skeleton, an RTV silicone by RS (692-542) was used.

To predict the initial shape of the bended structure and design the geometry, it was necessary to conduct three dimensional finite element analysis in ABAQUS CAE. Within this iterative process, the skeleton geometry was improved step wise and the membrane pre-strain was varied until a sufficient deformation was achieved.

Figure 4 depicts the initial design of the anisotropic silicone skeleton. It consisted of a rectangular base of height h, width W and length L, possessing a rectangular cavity of the length l and width w in which the DEA was placed. To create anisotropic bending stiffness, n rectangular bars of height H and width a were arranged on top of the base spaced by a distance of b. Figure 4 A depicts a drawing of the skeleton with all geometric measures, figure 4 B a three dimensional CAD model generated in SolidWorks. The chosen design possesseD numerous geometric values that could be adjusted to set the bending anisotropy, the general bending stiffness and the final bending curvature.

The silicone skeleton was meshed using three dimensional C3D20RH elements and the DE membrane was meshed using three dimensional M3D8R membrane elements. Both structures were modelled as hyper elastic, incompressible material using Yeoh's strain energy functions.[37] The material properties used and relevant references are given in table 1. Starting with an initial design similar to the one depicted in figure 4, DE

Table 1. Material properties used in ABAQUS CAE finite element model

Part	Material	Constants in MPa
Silicone skeleton	Sylgard 184 (1:10)	$C_{10} = 0.29$, $C_{20} = 0.015$, $C_{30} = 0.019$[38]
DE membrane	Wacker Elastosil 2030	$C_{10} = 0.1811$, $C_{20} = -0.01598$, $C_{30} = 0.00629$[39]

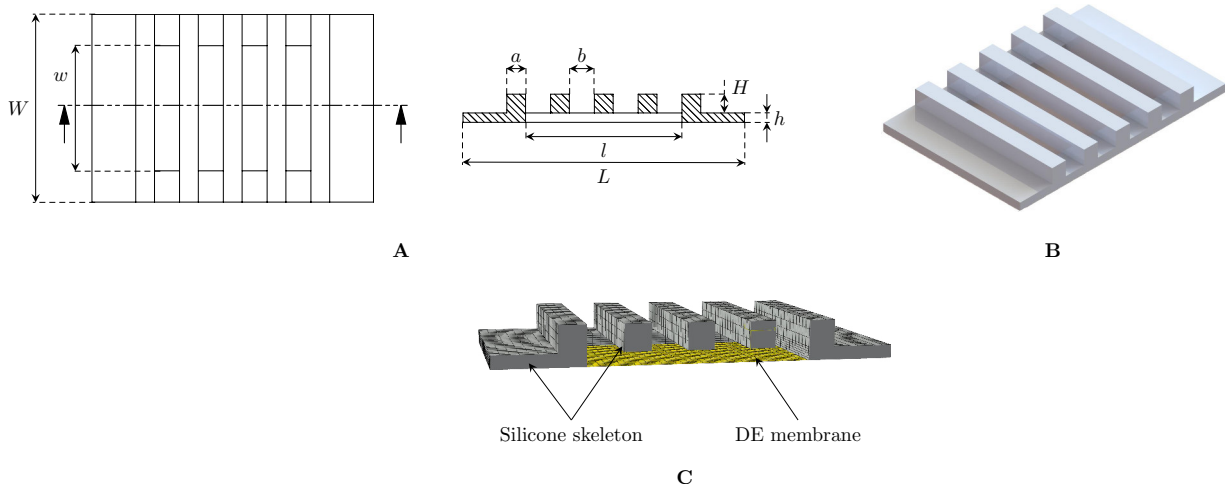

Figure 4. Initial design of an anisotropic bending stiffness structure for a soft robotic crawler. (A) Drawing, (B) three dimensional CAD model, (C) three dimensional finite element model (view cut) generated in ABAQUS based on the design depicted in figure 3.

membranes with different initial thickness and pre-strain were bonded in ABAQUS and the resulting deformation was calculated. The pre-strain was included in the simulation by applying initial stress to the membrane. To calculate this stress, an analytical calculation was conducted in advance.

Considering an equi-biaxial pre-strain λ_{pre} in the membrane, the resulting stress and remaining thickness t in the membrane were calculated using YEOH's strain energy density function:[37]

$$W = C_{10}(I_1 - 3) + C_{20}(I_1 - 3)^2 + C_{30}(I_1 - 3)^3, \tag{2}$$

where W is the strain energy density, $C_{10}\, C_{20}\, C_{30}$ the material properties and I_1 the first invariant of the left CAUCHY-GREE deformation tensor $\mathbf{b}$ and can be expressed as using the three principle stretches:

$$I_1 = \lambda_1^2 + \lambda_2^2 + \lambda_3^2. \tag{3}$$

For an incompressible, isotropic material, the principle stetches upon an introduced strain can be calculated by a derivation of the strain energy density function with respect to the principle stretches, taking into account the hydrostatic pressure p:[40]

$$\sigma_i = -p + \lambda_i \frac{\partial W(\lambda_i)}{\partial \lambda_i}. \tag{4}$$

In the developed structure the membrane was modelled as perfectly incompressible and was be pre-strained equi-biaxially. This yields the boundary conditions:

$$\lambda_1 = \lambda_2 = \lambda, \quad \lambda_3 = \frac{1}{\lambda^2}, \quad \sigma_3 = 0, \tag{5}$$

and results ins the equations:

$$p = \lambda_3 \frac{\partial W(\lambda_3)}{\partial \lambda_3}, \tag{6}$$

$$\sigma_2 = \sigma_1 = \sigma = -p + \lambda \frac{\partial W(\lambda)}{\partial \lambda}. \tag{7}$$

Combining equations 6 and 7 yields the strain in an equi-biaxially pre-strained, incompressible, hyper elastic membrane, according to YEOH's large strain theory:

$$\sigma = 2\left(\lambda^2 - \frac{1}{\lambda^4}\right)\left(C_{10} + 2C_{20}\left(s\lambda^2 + \frac{1}{\lambda^4} - 3\right) + 3C_{30}\left(s\lambda^2 + \frac{1}{\lambda^4} - 3\right)^2\right). \quad (8)$$

By using the material properties presented in table 1, resulting pre-strains generated by a certain stretch λ were calculated using equation 8. The general relation is depicted in figure 5 within the targeted pre-stretch range. It follows the typical characteristics for hyperelastic materials, showing a non-linear stress-stretch characteristic and a stretch-stiffening for large stretches. The chart also represents the thickness t of the membrane according to a certain pre-stretch, starting at the initial thickness $t_0 = 100\,\mu m$, following the function $t = t_0\lambda^{-2}$. This value is also important for the finite element model to implement the initial membrane conditions. During an

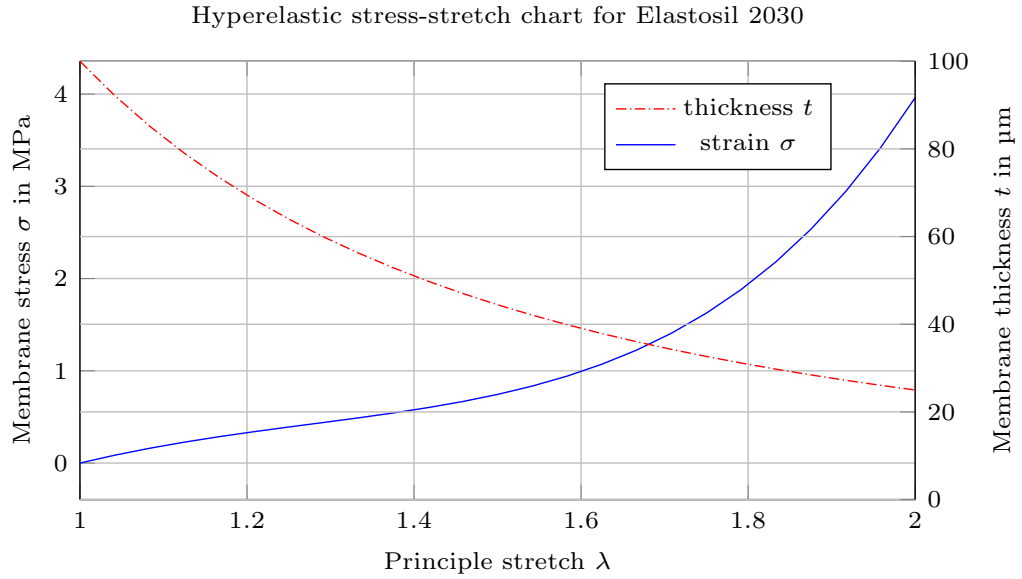

Figure 5. Stress-stretch chart for a hyperelastic Wacker Elastosil 2030 membrane according to a YEOH strain energy density function under equi-biaxial pre-strain.

iterative design and optimization process, a functional geometry design was derived by evaluating the resulting deformation of an assembly of a $\lambda = 1.75$ pre-stretched membrane and a silicone skeleton. The final chosen geometry values are presented in table 2. The pre-strain within the membrane has major impact on the final

Table 2. Geometric values of designed silicone skeleton regarding measures in figure 4

Measure	a	b	l	L	w	W	h	H
Value in mm	6	8	50	90	40	60	3	6

shape and, thus, the operation of the whole structure. To illustrate this influence, several analyses using the chosen geometry and varying membrane pre-strains were carried out. The results are illustrated in figure 6. Depending on the amount of pre-strain, the structure bends anisotropically around the z-axis. The maximum deformation in y-direction around the z-axis was $\approx 35\,mm$. The y-deformation around the x-axis is comparably small. For the produced demonstrators, a pre-stress of $\lambda = 1.75$, resulting in a pre-strain $\sigma_{pre} = 1.625\,MPa$, was chosen (figure 6 boxed representation). This pre-stress is similar to the instantaneous pre-stress of a $\lambda = 3.5$ equi-biaxially pre-stretched VHB membrane ($\sigma_{pre}^{VHB} = 1.626\,MPa$). However, due to the viscoelastic relaxation

in a VHB membrane the remaining long term pre-stress after relaxation is only $\sigma_{\text{pre}'}^{\text{VHB}} = 0.523\,\text{MPa}$ and would result in only $\approx 15\,\text{mm}$ deformation.

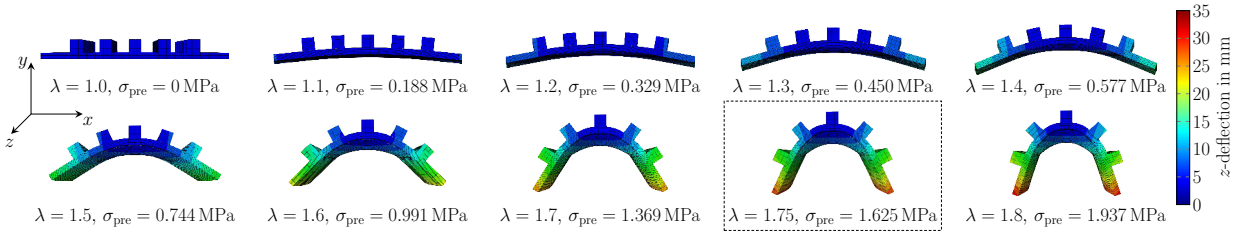

Figure 6. Representation of the influence of different membrane pre-strains on the deformation of the assembled system and the final chosen set-up (boxed).

2.3 Production technology

To assemble the bending structure, at first the silicone skeleton was mould cast, using a mould built up from several layers of laser cut PMMA (figure 7 A). The two components of the Sylgard 184 PDMS elastomer kit were mixed in a ratio of 10:1 and degassed in a vacuum chamber until all air bubbles were removed. Afterwards, the liquid silicone was injected using a syringe and cured at 80 °C for two hours.
The silicone membrane was pre-strained by $\lambda = 1.75$ (figure 7 B) using an iris-like stretching rig made of laser-cut PMMA. To apply the condutive, compliant electrodes to the membrane, an electrode ink, suitable to spray painting, was developed. To ensure a good electrode deposition, a recipe similar to the one presented by McCoul et al.[41] was adapted to the spray painting process. As silicone for the electrodes, Bluestar Silicones Silbione LSR 4305, a two part heat curing silicone, was used. 2 g of each part were mixed with 0.4 g carbon black (Vulcan XC-72R) and 12g of each isopropanol and isooctane. The ink was mixed for 5:30 min in a planetary mixer (Thinky ARE-250CE). To apply the electrode ink to the membrane, a commonly used air brush and a laser cut PET stencil was used (figure 7 C). For bonding the silicone skeleton to the membrane, a thin film of RTV silicone by RS (692-542) was applied using a razor blade to the bottom of the skeleton, and the skeleton was pressed to the membrane for 30 min (figure 7 D). Afterwards, the structure was cut out with a scalpel (figure 7 E) and the bottom electrode was spray painted using an air brush again. Finally the entire assembly is cured at 150 °C for two hours.

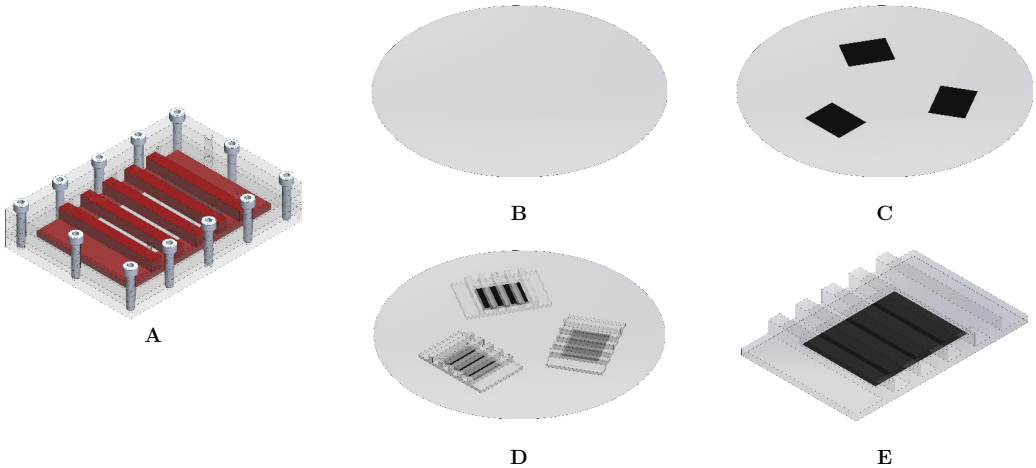

Figure 7. Production of entirely soft DE bending structure: (A) mould casting of silicone skeleton (false color representation), (B) pre-strained silicone membrane, (C) spray painted electrodes, applied by an air brush using stencils, (D) bonding of silicone skeletons to the membrane, (E) final structure (undeformed).

3. RESULTS AND DISCUSSION

In the presented paper we summarized possible applications of DEs in soft robots and robotic structures, utilizing their multifunctional properties, on the basis of examples developed in our lab. The combination of soft DE -actuators, -sensors, -signal processors, -signal generators and energy harvesters opens up the possibility to produce all functional sub units of a classic robotic system by only using two materials: soft silicone and carbon. So far the the design based on DEs was limited to partly soft systems, since rigid structures for maintaining the necessary pre-strain in the membrane were essential. We presented a novel design to combine soft DE membranes with soft silicone skeletons that can maintain the membrane strains and are soft at the same time. Figure 8 depicts the results of a FE analysis of the final design and a photograph of the same, fully assembled and cured. The FE simulation did not take into account the mass of the structure at this point. That resulted in a slight difference in the total deformation, since the real structure deformed itself under its own gravitational force. Furthermore, we observed a variation of bending curvature from batch to batch. We assume that this was due to the huge impact of small variations in the mixing ratio of the two liquid components of the silicone used for the skeleton. Additionally within the pre-stretch range applied to the membrane, small changes in pre-strain had a large impact on the generated pre-stress and, thus, the final bending curvature. With respect to the used pre-stretching technology we estimate a systematic error of $\Delta\lambda = 0.05$ which results in uncertainty of pre-stress $\sigma_{\text{pre}} = 1.491\,\text{MPa}...1.774\,\text{MPa}$. To prove the functionality of the whole structure, it was supplied by oscillating

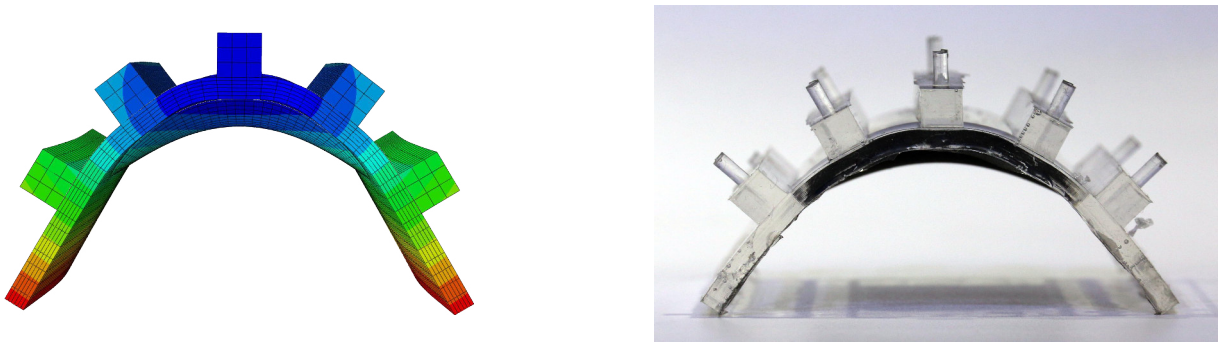

A **B**

Figure 8. Entirely soft DE bended crawling structure. (A) FE model of reached deformation upon chosen pre-stess in the DE membrane. (B) Photograph of a sample structure.

voltage signals of different frequencies generated by a high voltage signal controller. The first results are shown in the video supplied by the link given in figure 9. It demonstrated the silicone structure upside down in its *jumping*-mode, in its desired *crawling*-mode and integrated in a *flapping wing* dragonfly-like device. Depending on the resonant frequency in every mode, large actuation can be generated. To demonstrate the full potential of multifunctional DEs for soft robotic applications, an entirely soft, autonomous, crawling structure will be presented in the next study. A DEO will be integrated into the fully soft structure and will autonomously run a crawling robot that will only be supplied by an external DC voltage. All signal processing and driving DE electronics, consisting of nothing more than carbon and silicone will be integrated in that structure.

ACKNOWLEDGMENTS

This project has received funding from the European Unions Horizon 2020 research and innovation programme under the Marie Sklodowska-Curie grant agreement No 706754.

REFERENCES

[1] Majidi, C., "Soft robotics: a perspectivecurrent trends and prospects for the future," *Soft Robotics* **1**(1), 5–11 (2014).

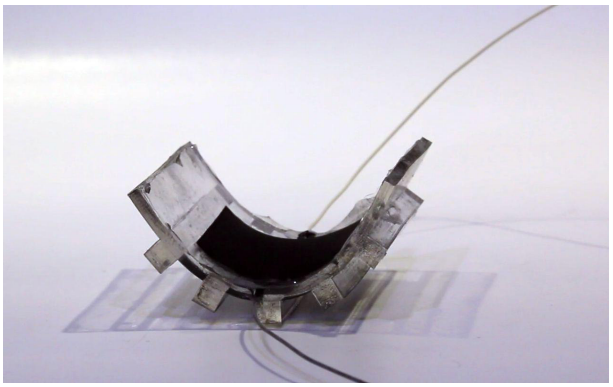

Figure 9. Video 1: A video of the developed entirely soft DE robotic structure in different application modes: http://dx.doi.org/10.1117/12.2260361.1

[2] Trivedi, D., Rahn, C. D., Kier, W. M., and Walker, I. D., "Soft robotics: Biological inspiration, state of the art, and future research," *Applied Bionics and Biomechanics* **5**(3), 99–117 (2008).

[3] Suzumori, K., Iikura, S., and Tanaka, H., "Applying a flexible microactuator to robotic mechanisms," *Control Systems, IEEE* **12**(1), 21–27 (1992).

[4] Chou, C.-P. and Hannaford, B., "Measurement and modeling of mckibben pneumatic artificial muscles," *Robotics and Automation, IEEE Transactions on* **12**(1), 90–102 (1996).

[5] Shepherd, R. F., Ilievski, F., Choi, W., Morin, S. A., Stokes, A. A., Mazzeo, A. D., Chen, X., Wang, M., and Whitesides, G. M., "Multigait soft robot," *Proceedings of the National Academy of Sciences* **108**(51), 20400–20403 (2011).

[6] Katzschmann, R. K., Marchese, A. D., and Rus, D., "Hydraulic autonomous soft robotic fish for 3d swimming," in [*Experimental Robotics*], 405–420, Springer (2016).

[7] Calisti, M., Giorelli, M., Levy, G., Mazzolai, B., Hochner, B., Laschi, C., and Dario, P., "An octopus-bioinspired solution to movement and manipulation for soft robots," *Bioinspiration & biomimetics* **6**(3), 036002 (2011).

[8] Laschi, C., Cianchetti, M., Mazzolai, B., Margheri, L., Follador, M., and Dario, P., "Soft robot arm inspired by the octopus," *Advanced Robotics* **26**(7), 709–727 (2012).

[9] Rogers, J. A., Someya, T., and Huang, Y., "Materials and mechanics for stretchable electronics," *Science* **327**(5973), 1603–1607 (2010).

[10] Rus, D. and Tolley, M. T., "Design, fabrication and control of soft robots," *Nature* **521**(7553), 467–475 (2015).

[11] Tolley, M. T., Shepherd, R. F., Mosadegh, B., Galloway, K. C., Wehner, M., Karpelson, M., Wood, R. J., and Whitesides, G. M., "A resilient, untethered soft robot," *Soft Robotics* **1**(3), 213–223 (2014).

[12] Marchese, A. D., Onal, C. D., and Rus, D., "Autonomous soft robotic fish capable of escape maneuvers using fluidic elastomer actuators," *Soft Robotics* **1**(1), 75–87 (2014).

[13] Bartlett, N. W., Tolley, M. T., Overvelde, J. T. B., Weaver, J. C., Mosadegh, B., Bertoldi, K., Whitesides, G. M., and Wood, R. J., "A 3d-printed, functionally graded soft robot powered by combustion," *Science* **349**(6244), 161–165 (2015).

[14] Wehner, M., Truby, R. L., Fitzgerald, D. J., Mosadegh, B., Whitesides, G. M., Lewis, J. A., and Wood, R. J., "An integrated design and fabrication strategy for entirely soft, autonomous robots," *Nature* **536**, 451–455 (aug 2016).

[15] Pelrine, R. E., Kornbluh, R. D., and Joseph, J. P., "Electrostriction of polymer dielectrics with compliant electrodes as a means of actuation: Tenth ieee international workshop on micro electro mechanical systems," *Sensors and Actuators A: Physical* **64**(1), 77–85 (1998).

[16] Bar-Cohen, Y., "Electroactive polymers as artificial muscles: A review," *Journal of Spacecraft and Rockets* **39**(6), 822–827 (2002).

[17] Carpi, F., De Rossi, D., Kornbluh, R., Pelrine, R. E., and Sommer-Larsen, P., [*Dielectric elastomers as electromechanical transducers: Fundamentals, materials, devices, models and applications of an emerging electroactive polymer technology*], Elsevier (2011).

[18] Anderson, I. A., Gisby, T. A., McKay, T. G., OBrien, B. M., and Calius, E. P., "Multi-functional dielectric elastomer artificial muscles for soft and smart machines," *Journal of Applied Physics* **112**(4), 041101 (2012).

[19] Pelrine, R., Kornbluh, R., Pei, Q., and Joseph, J., "High-speed electrically actuated elastomers with strain greater than 100%," *Science* **287**(5454), 836–839 (2000).

[20] Li, T., Keplinger, C., Baumgartner, R., Bauer, S., Yang, W., and Suo, Z., "Giant voltage-induced deformation in dielectric elastomers near the verge of snap-through instability," *Journal of the Mechanics and Physics of Solids* **61**(2), 611–628 (2012).

[21] Toth, L. A. and Goldenberg, A. A., "Control system design for a dielectric elastomer actuator: the sensory subsystem," *Proc. SPIE* **4695**, 323–334 (2002).

[22] Keplinger, C., Kaltenbrunner, M., Arnold, N., and Bauer, S., "Capacitive extensometry for transient strain analysis of dielectric elastomer actuators," *Applied Physics Letters* **92**(19), 192903 (2008).

[23] Gisby, T., Xie, S., Calius, E., and Anderson, I., "Integrated sensing and actuation of muscle-like actuators," in [*Proc. SPIE 7287*], 728707–728707, International Society for Optics and Photonics (2009).

[24] O'Brien, B., Gisby, T., Xie, S. Q., Calius, E., and Anderson, I., "Biomimetic control for dea arrays," in [*Proc. SPIE 7642*], 764220–764220, International Society for Optics and Photonics (2010).

[25] O'Brien, B., Gisby, T., and Anderson, I. A., "Stretch sensors for human body motion," in [*Proc. SPIE 9056*], 905618–905618, International Society for Optics and Photonics (2014).

[26] O'Brien, B. M., Calius, E. P., Inamura, T., Xie, S. Q., and Anderson, I. A., "Dielectric elastomer switches for smart artificial muscles," *Applied Physics A* **100**(2), 385–389 (2010).

[27] O'Brien, B. M. and Anderson, I. A., "An artificial muscle ring oscillator," *Mechatronics, IEEE/ASME Transactions on* **17**(1), 197–200 (2012).

[28] O'Brien, B. M., McKay, T. G., Gisby, T. A., and Anderson, I. A., "Rotating turkeys and self-commutating artificial muscle motors," *Applied Physics Letters* **100**(7), 074108 (2012).

[29] McKay, T. G., OBrien, B. M., Calius, E. P., and Anderson, I. A., "Soft generators using dielectric elastomers," *Applied Physics Letters* **98**(14), 142903 (2011).

[30] Wilson, K. E., Henke, E.-F. M., Slipher, G. A., and Anderson, I. A., "Rubbery logic gates," *Extreme Mechanics Letters* **9**, 188 – 194 (2016).

[31] Wilson, K. E., Henke, E.-F. M., Slipher, G. A., and Anderson, I. A., "Rubbery computing," in [*Proc. SPIE*], Bar-Cohen, Y., ed., **10163**, SPIE (apr 2017).

[32] O'Brien, B. M. and Anderson, I. A., "An artificial muscle computer," *Applied Physics Letters* **102**(10), 104102 (2013).

[33] Kofod, G., Sommer-Larsen, P., Kornbluh, R., and Pelrine, R., "Actuation response of polyacrylate dielectric elastomers," *Journal of Intelligent Material Systems and Structures* **14**(12), 787–793 (2003).

[34] Henke, E.-F. M., Schlatter, S., and Anderson, I. A., "A soft electronics-free robot," *CoRR* **abs/1603.05599** (2016).

[35] Henke, E.-F. M., Schlatter, S., and Anderson, I. A., "Soft dielectric elastomer oscillators driving bioinspired robots," *Soft Robotics* (2017). In press.

[36] Zhao, J., Wang, S., McCoul, D., Xing, Z., Huang, B., Liu, L., and Leng, J., "Bistable dielectric elastomer minimum energy structures," *Smart Materials and Structures* **25**(7), 075016 (2016).

[37] Yeoh, O. H., "Some forms of the strain energy function for rubber," *Rubber Chemistry and Technology* **66**(5), 754–771 (1993).

[38] Lü, C., Li, M., Xiao, J., Jung, I., Wu, J., Huang, Y., Hwang, K.-C., and Rogers, J. A., "Mechanics of tunable hemispherical electronic eye camera systems that combine rigid device elements with soft elastomers," *Journal of Applied Mechanics* **80**, 061022 (aug 2013).

[39] Kuhring, S., Uhlenbusch, D., Hoffstadt, T., and Maas, J., "Finite element analysis of multilayer DEAP stack-actuators," in [*Proc. SPIE 9430*], Bar-Cohen, Y., ed., 94301L (2015).

[40] Holzapfel, G. A., [*Nonlinear solid mechanics: A continuum approach for engineering*], Wiley, Chichester, Weinheim [u.a.] (2010).

[41] McCoul, D., Rosset, S., Besse, N., and Shea, H., "Multifunctional shape memory electrodes for dielectric elastomer actuators enabling high holding force and low-voltage multisegment addressing," *Smart Materials and Structures* **26**(2), 025015 (2017).